

Revertants, Low Temperature, and Correctors Reveal the Mechanism of F508del-CFTR Rescue by VX-809 and Suggest Multiple Agents for Full Correction

Carlos M. Farinha,¹ John King-Underwood,² Marisa Sousa,¹ Ana Raquel Correia,³ Bárbara J. Henriques,³ Mónica Roxo-Rosa,¹ Ana Carina Da Paula,^{1,4} Jonathan Williams,² Simon Hirst,² Cláudio M. Gomes,³ and Margarida D. Amaral^{1,*}

¹Faculty of Sciences, Center for Biodiversity, Functional, and Integrative Genomics, University of Lisboa, Campo Grande, 1749-016 Lisboa, Portugal

²Sygnature Discovery, BioCity, Nottingham NG1 1GF, UK

³Instituto de Tecnologia Química e Biológica, Universidade Nova de Lisboa, Av. República, 2780-157 Oeiras, Portugal

⁴Present address: Department of Cell Biology and Physiology, School of Medicine, University of Pittsburgh, Pittsburgh, PA 15224, USA

*Correspondence: mdamaral@fc.ul.pt

<http://dx.doi.org/10.1016/j.chembiol.2013.06.004>

SUMMARY

Cystic fibrosis is mostly caused by the F508del mutation, which impairs CFTR protein from exiting the endoplasmic reticulum due to misfolding. VX-809 is a small molecule that rescues F508del-CFTR localization, which recently went into clinical trial but with unknown mechanism of action (MoA). Herein, we assessed if VX-809 is additive or synergistic with genetic revertants of F508del-CFTR, other correctors, and low temperature to determine its MoA. We explored and integrated those various agents in combined treatments, showing how they add to each other to identify their complementary MoA upon correction of F508del-CFTR. Our experimental and modeling data, while compatible with putative binding of VX-809 to NBD1:ICL4 interface, also indicate scope for further synergistic F508del-CFTR correction by other compounds at distinct conformational sites/cellular checkpoints, thus suggesting requirement of combined therapies to fully rescue F508del-CFTR.

INTRODUCTION

Cystic fibrosis (CF), the most common autosomal recessive disease among Caucasians, is caused by mutations in the gene encoding the CF transmembrane conductance regulator (CFTR) protein (Riordan et al., 1989). The most prevalent mutation F508del occurs in more than 90% of CF patients (Riordan et al., 1989), so most CF therapeutic efforts focus on the correction of this mutant.

CFTR possesses two transmembrane domains (TMD1/2), two nucleotide binding domains (NBD1/2)—which bind and hydrolyse ATP, regulating the gating of the channel—and a regulatory domain (RD), with multiple phosphorylation sites (Riordan, 2008).

The F508del mutation causes CFTR to fail in reaching its proper location at the plasma membrane (PM), instead being mostly retained at the endoplasmic reticulum (ER) from where it

is rapidly sent to proteasomal degradation (Jensen et al., 1995). Although failure in acquiring a native conformation is accepted as the major cause for ER retention of F508del-CFTR, ultimately it is the cellular machinery called the ER quality control (ERQC) that actively disqualifies F508del-CFTR from exiting the ER (Farinha and Amaral, 2005; Jensen et al., 1995). Our initial model of the ERQC (Farinha and Amaral, 2005) proposed two checkpoints involving the distinct Hsp70/Hsc70 and calnexin chaperone machineries, sequentially assessing the folding status of CFTR and targeting for degradation nonnative protein conformation forms (reviewed in Amaral, 2004, 2011). Later, we postulated a third ERQC checkpoint controlling CFTR ER export (Roxo-Rosa et al., 2006), whereby misfolded F508del-CFTR fails to exit the ER due to exposure of ER retention motifs—four arginine-framed (RXR) tripeptides (AFTs)—whose substitution leads to F508del-CFTR rescue (Chang et al., 1999; Roxo-Rosa et al., 2006). In contrast, active ER export of WT-CFTR relies on the presence of a diacidic code (NBD1-located “DAD” motif), a cargo signal for Sec24-mediated COPII packing (Nishimura and Balch, 1997). Wang et al. (2004) showed that alanine-substitution of the second “DAD” Asp-residue in CFTR reduced both its Sec24-CFTR association and ER exit. Additional evidence supports DAA-CFTR as a trafficking mutant without a major conformational defect in contrast to F508del-CFTR, a conformational mutant with a partially functional ER exit code (Roy et al., 2010).

Besides such cellular mechanisms (cell autonomous), F508del-CFTR is also prevented from reaching the cell surface because of its intrinsic abnormal folding (protein autonomous) caused by at least three major defects. First, isolated CFTR F508del-NBD1 has an intrinsic folding defect, as shown by (1) impaired F508del-NBD1 folding kinetics versus wild-type(WT)-NBD1 (Qu and Thomas, 1996), (2) ability of some NBD1 amino acid variants to both solubilize isolated F508del-NBD1 in vitro and also to rescue in vivo full-length F508del-CFTR to the PM (Pissarra et al., 2008), and (3) demonstration by surface-plasmon resonance that F508del-NBD1 is a potent substrate of Hsp70 with 5-fold higher affinity than the WT domain (Scott-Ward and Amaral, 2009).

The second F508del-associated defect impairs CFTR interdomain folding, namely, (1) the NBD1-NBD2 dimerization interface (critical for channel activation and accounting for the F508del-CFTR gating defect; Dalemans et al., 1991), which can be

rescued by the G550E revertant, and (2) the interaction of NBD1 with the fourth intracellular loop (ICL4) of TMD2 (Serohijos et al., 2008), shown to be reverted by either V510D (Loo et al., 2010) or R1070W, which both fill the pocket left empty by F508del (Thibodeau et al., 2010).

Third, when rescued F508del-CFTR reaches the cell surface, it still presents a reduced half-life (Lukacs et al., 1993; Sharma et al., 2001), due to both reduced recycling (Sharma et al., 2004) and increased endocytosis (Swiatecka-Urban et al., 2005). The latter was recently shown to be corrected by Rac1 signaling and HGF (Moniz et al., 2013).

Altogether, these protein-autonomous defects account for the much reduced function of ER-rescued F508del-CFTR as a Cl⁻ channel in comparison to its WT counterpart (Dalemans et al., 1991). Efforts have thus been put into high-throughput screening of small molecule libraries to identify correctors (Pedemonte et al., 2005) that rescue F508del-CFTR to the cell surface, among which VX-809 is already in late-stage clinical trials (Van Goor et al., 2011). Despite its impressive rescue levels in primary cultures of CF patients' lung cells, the success of this compound in F508del-homozygous patients is modest (Clancy et al., 2012), and its mechanism of action (MoA) has only very recently begun to be understood (He et al., 2013; Okiyoneda et al., 2013). Previous correctors (e.g., Corr-4a, VRT-325) showed limited rescue of F508del-CFTR, probably due to action exerted at one of the multiple mutant defects (Grove et al., 2009; Varga et al., 2008).

Herein, we explored the MoA of VX-809 by analyzing its synergistic/additive effect with those of previously characterized genetic revertants, which rescue F508del-CFTR by causing different effects: 4RK affecting traffic (Roxo-Rosa et al., 2006), G550E (Roxo-Rosa et al., 2006) and R555K increasing channel gating by strengthening the NBD1:NBD2 dimer interface, and R1070W (Serohijos et al., 2008) and V510D (Wang et al., 2007a; Loo et al., 2010) by filling the NBD1:ICL4 interface. Finally, we also tested VX-809 together with low temperature (Denning et al., 1992) and the Corr-4a, VRT-325 correctors.

Our data show that VX-809 and the two other correctors exert variable effects on the genetic revertants and support VX-809 putative binding at the interface of NBD1 with TMD2 ICL4 consistently with our modeling data and recent findings from others published while this paper was under review (He et al., 2013; Okiyoneda et al., 2013). Interestingly, VX-809 adds up to the two other correctors in the rescue of F508del-CFTR and also with low temperature. Altogether, these data lead us to conclude that there is scope for correction beyond VX-809 at distinct F508del-CFTR conformational sites/cellular folding checkpoints. Moreover, combined therapeutic strategies to rescue F508del-CFTR may be required to reach the threshold of functional CFTR necessary to avoid CF.

RESULTS

VX-809 Fails to Promote Folding of Isolated F508del-NBD1

To assess the thermal stability of murine CFTR NBD1 (either WT- or F508del) in the presence of chemical correctors, we used differential scanning fluorimetry (DSF), which monitors the thermal

unfolding of the protein in the presence of fluorescent Sypro Orange dye (Niesen et al., 2007). As the dye is highly sensitive to nonpolar environments (exposed during unfolding), fluorescence also increases with protein unfolding. By plotting fluorescence intensity as a function of temperature, a sigmoidal curve describing a two-state transition (Figure S1 available online) is generated, and the inflection point of the transition curve corresponds to the melting temperature (T_m). The traces corresponding to the control experiments already point to a higher destabilization of murine F508del- versus WT-NBD1, due to both lower T_m and also higher initial dye intensity, indicative of a less compact fold. The assays with VX-809, VRT-325, and Corr-4a correctors (using a protein:compound 1:1 stoichiometry) did not reveal any potential of NBD1 stabilization (Table S1). Notwithstanding, a preliminary study with VX-809 suggests that it may exert an effect on the reorganization of the NBD1 fold, as it decreases Sypro binding intensity at 37°C (C.M.G., unpublished data). Although this effect does not increase the domain thermodynamic stability, it effectively modulates its unfolding kinetics.

VX-809 Adds to VRT-325 and Corr-4a to Rescue F508del-CFTR but Exhibits Variable Effects on Genetic Revertants

In order to characterize the rescue mechanism of VX-809 on F508del-CFTR, we then tested the effect of incubating it together with VRT-325 and Corr-4a on BHK cells stably expressing this mutant alone or in *cis* with the following genetic revertants: (1) 4RK (where the four AFTs were simultaneously mutated to lysines), (2) G550E, (3) R1070W, (4) V510D, or (5) R555K (Figures 1A–1E). Processing of each CFTR variant was assessed by western blot (WB; Figures 1A–1E) and measured as the percentage of fully processed (band C) to total CFTR (band C + immature form band B) and then normalized to the same WT-CFTR ratio (Figure 1F).

Incubation with each of the compounds VX-809, Corr-4a, or VRT-325 led to the appearance of fully processed F508del-CFTR, as previously (Loo et al., 2005; Pedemonte et al., 2005; Van Goor et al., 2011) albeit with different efficacy: 24%, 9%, and 19%, respectively. Furthermore, data analysis shows that VX-809 rescue of F508del-CFTR adds to that by Corr-4a or VRT-325 and also to that of the two latter compounds together (Figures 1A and 1G), suggesting that these three small molecules act by distinct MoA. Some rescue of F508del-CFTR by DMSO acting as a chemical chaperone was also detected as previously noted by many others (see, e.g., Pedemonte et al., 2005; Varga et al., 2008).

Interestingly, however, analysis of the effects of the three compounds upon the revertants showed that VX-809 (but neither VRT-325 nor Corr-4a) is additive to G550E or R555K in correcting F508del-CFTR (by 38% and 32%, respectively), strongly suggesting that VX-809 acts differently from these two revertants. Moreover, whereas both VRT-325 and VX-809 add significantly to the effect of R1070W by ~17% ($p = 0.011$) and 28% ($p = 1.6 \times 10^{-5}$), respectively, Corr-4a does not. In contrast, all the three compounds produce a significant increase in the amount of processed F508del-4RK-CFTR (Figure 1G), suggesting that 4RK acts differently. Curiously, all the three compounds further increase band C levels of F508del-V510D-CFTR, but VRT-325 produces the greatest effect.

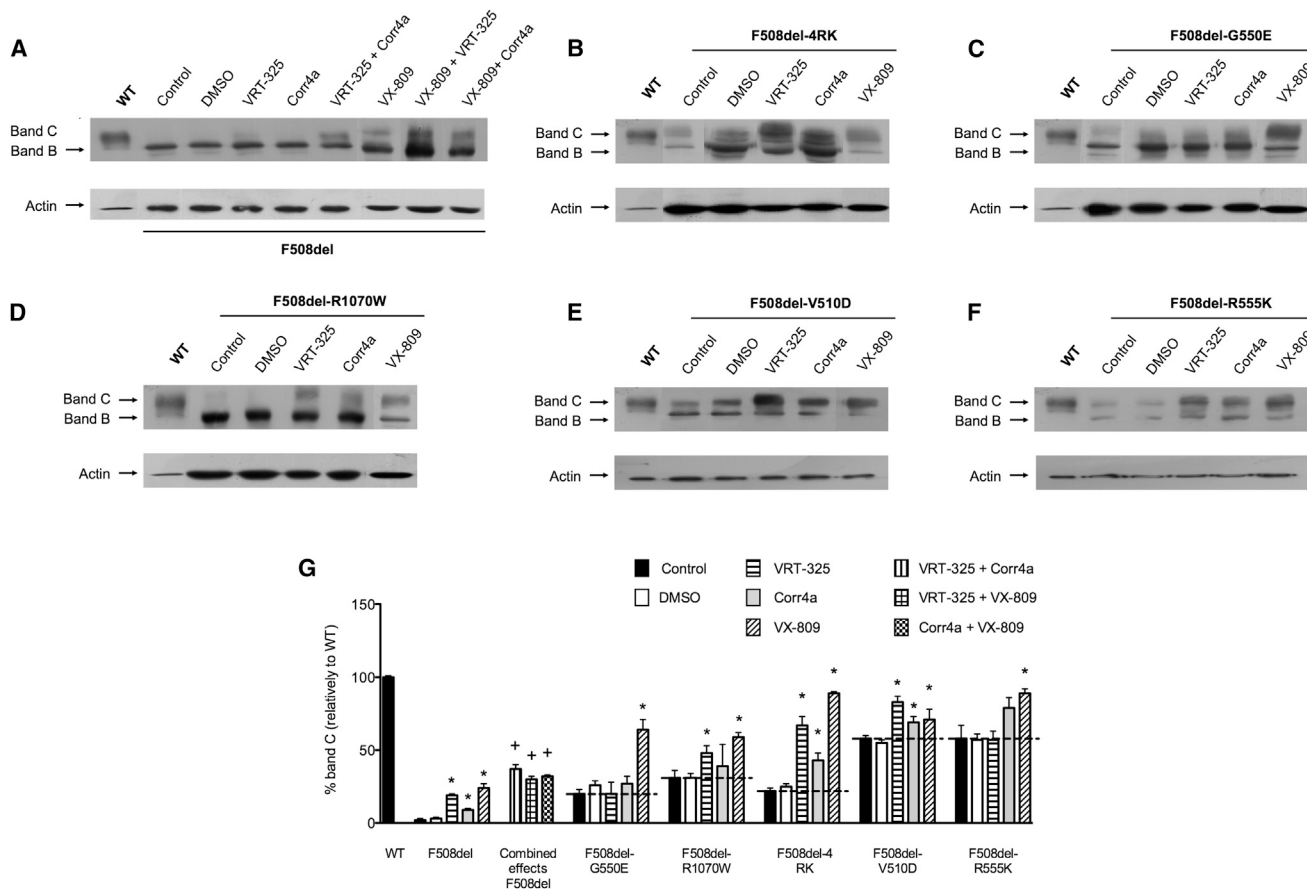


Figure 1. Effect of Small Molecule Correctors on F508del-CFTR and Genetic Revertants

(A–F) BHK cell lines stably expressing CFTR bearing F508del alone (A) or in cis with 4RK (B), G550E (C), R1070W (D), V510D (E), and R555K (F) were incubated for 24 hr with 6.7 μ M VRT-325, 10 μ M Corr-4a, or 3 μ M VX-809 alone or in combination. CFTR protein was analyzed by western blot with the anti-CFTR 596 mAb. Data are representative of $n = 7$ independent experiments.

(G) For each condition, densitometry was used to calculate the percentage of band C to total CFTR expressed. Data were normalized to WT-CFTR and are shown as mean \pm SEM. Asterisks indicate significant difference from the same CFTR variant with DMSO ($p < 0.05$). Dotted lines correspond to levels of band C in revertants without treatment.

See also Figure S1 and Table S1.

Potency of Correctors in Increasing Processing of Revertants

To further understand the effect of the small molecule compounds on the genetic revertants, we analyzed the dose response of processing by the correctors (Figures 2A–2C). These analyses were performed for three of the revertants with different F508del-CFTR effects (4RK, traffic; G550E, NBD1:NBD2 dimer interface; and R1070W, NBD1:ICL4 interface).

Results show that, in general, much lower corrector concentrations are needed to increase revertants processing in comparison to those required to rescue F508del-CFTR. For example, an increase in F508del-G550E-CFTR processing is detected at 0.3 μ M VX-809, whereas a 10-fold higher concentration is needed for significant rescue of F508del-CFTR (Figure 2C).

Additive Effects of Small Molecule Correctors and Low Temperature

To shed more light on the MoA of F508del-CFTR rescue by VX-809, we next tested its effects (and the effects of VRT-325 and

Corr-4a) under low temperature by incubating cells for 48 hr at 26°C alone or in the presence of each corrector (or DMSO control) for the last 24 hr (Figures 2D and 2E).

Additive/synergistic effects on F508del-CFTR rescue were detected between each corrector and low temperature. Rescue of F508del-CFTR by VX-809 at 26°C reached $\approx 80\%$ of WT-CFTR processing, i.e., an additional (statistically significant) $\approx 40\%$ increase compared to low temperature alone, whereas VRT-325 and Corr-4a at 26°C reached $\approx 60\%$ of WT-CFTR (Figure 2E). These data suggest that low temperature acts on F508del-CFTR differently from the three correctors.

CFTR Modeling

To better understand our experimental findings, we modeled CFTR (Figure 3) based on the published NBD1 X-ray data (Lewis et al., 2010). The full protein was modeled based on the structure of Sav1866 (Hohl et al., 2012). Where such data were not available, we resorted to constructing homology models.

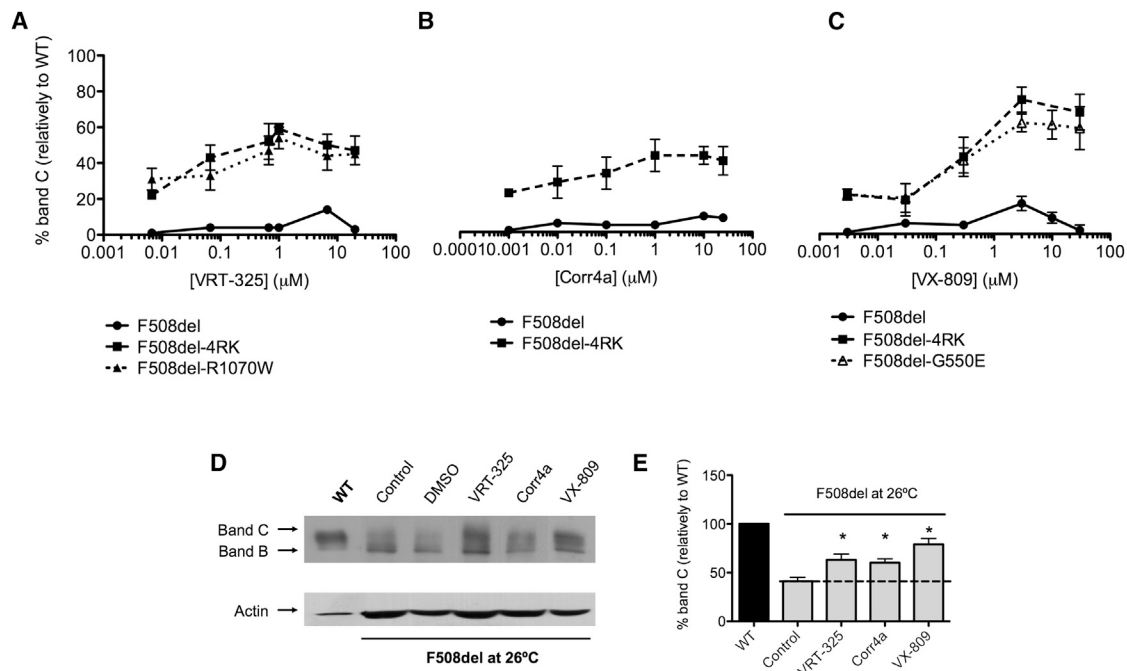


Figure 2. Potency of Correctors on Genetic Revertants and with Low Temperature

(A–C) BHK cell lines stably expressing CFTR bearing F508del alone or in cis with the indicated genetic revertants were incubated for 24 hr with (A) 6.7, 67, and 670 nM and 1, 6.7, or 20 μM VRT-325, (B) 1, 10, and 100 nM and 1, 10, or 25 μM Corr4a, or (C) 3, 30, and 300 nM and 3, 10, or 30 μM VX-809. CFTR protein was analyzed by western blot with the anti-CFTR 596 mAb. Data are representative of $n = 4$ independent experiments. For each condition, densitometry was used to calculate the percentage of band C to total CFTR expressed. Data were normalized to WT-CFTR and are shown as mean \pm SEM.

(D) BHK cell lines stably expressing CFTR bearing F508del were incubated for 48 hr at 26°C along with VRT-325, Corr-4a, or VX-809 for the final 24 hr. CFTR protein was analyzed by WB.

(E) Percentage of band C versus total CFTR. Asterisks indicate significant difference from the F508del-CFTR at 26°C under treatment with DMSO - control ($p < 0.05$). Dotted line corresponds to levels of band C in F508del-CFTR at 26°C.

Our full-length model (Figure 3A) depicts WT-CFTR without the RD and with ATP bound to the two sites (shown in space-filling mode) at the NBD1:NBD2 interface. It recapitulates critical interdomain interactions already predicted by others (Serohijos et al., 2008), identifying the proximity of the F508-containing NBD1 surface with ICL4 of TMD2 (Figure S2A).

To understand the structural differences between WT- and F508del-NBD1, we overlay published structures (2BBT and 2BBO, respectively) (Lewis et al., 2010) by sequence and secondary structure (Figure 3B). As previously shown, the most evident difference is the absence of the aromatic ring of F508 at the surface of the mutant domain. Further, the overlay of the two domains allows the identification of a significant difference in the 573–580 loop (as highlighted in the lower inset, Figure 3B), adjacent to Asp572 (Walker B). Still in this loop, Tyr577 interacts with ATP in WT-NBD1 but rearranges to a distal position in F508del-NBD1, contributing to a certain loosening of the mutant structure (Figure 3C).

Modeling of the NBD1:NBD2 heterodimer ATP site was based on the NBD1 homodimer structure (Protein Data Bank [PDB] ID code: 2PZE) (Atwell et al., 2010), in which one half was used as a template for overlay of NBD2 (PDB ID code: 3GD7). Further refinement of the overlay on the ATP sites yielded an authentic heterodimer model. These models allowed the search for differential contact sites (Figures 3D and 3E), and their analysis showed the presence of two contact sites in

WT-CFTR that are severely altered in F508del-CFTR: one corresponding to the previously described interaction of ICL4 and NBD1 (Serohijos et al., 2008) (also shown in Figure S2A) and the second to the interface of the two NBDs around the ATP sites.

We then assessed the effect of revertants G550E and R1070W by modeling (Figure 3F; Figures S2B and S2C), whereby G550E allows a salt bridge to form across the ATP binding site with Lys1250 and other residues from NBD2 (Figure 3F). By contrast, R1070W (Figure S2A) plausibly fills in the space left empty by absence of F508 at the NBD1:ICL4 interface as previously proposed (Thibodeau et al., 2010).

Investigation of the F508del-CFTR model using ligand binding site finding algorithm “Q-SiteFinder” led us to the strong likelihood that CFTR correctors or potentiators bind to one of two sites, namely, at the NBD1:NBD2 or the NBD1:ICL4 interfaces. Then, using docking and scoring techniques, to determine which of these two binding sites best accommodate correctors, we propose that, whereas VRT-325 is best accommodated by the ATP site at the NBD1:NBD2 interface (Figure 3G), VX-809 is a good fit for the pocket left empty by F508 at the NBD1:ICL4 interface (Figure 3H). We did not find a good fit for Corr-4a in either of these proposed sites. Although these putative binding sites resulted from our highest scoring results, we should acknowledge that there is some uncertainty associated with this modeling approach.

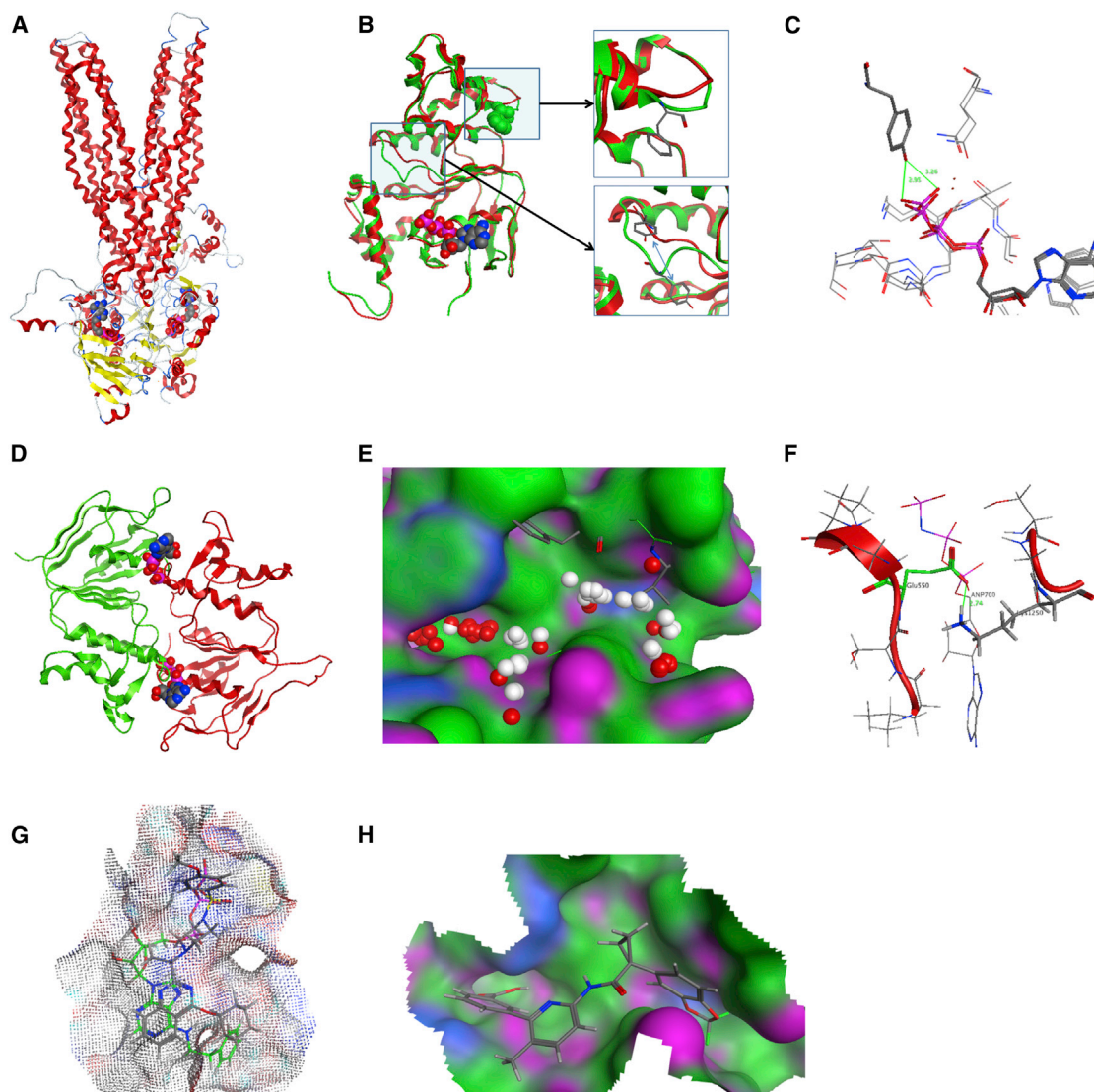


Figure 3. Modeling of CFTR Structure to Identify Critical Interactions as well as Similarities and Differences between WT- and F508del-NBD1

(A) Full model of WT-CFTR without R-domain and with ATP at both sites based on Sav1866.

(B) Overlay of WT- and F508del-NBD1 with the major differences highlighted.

(C) Interaction of loop 573-580 with ATP in WT-NBD1.

(D) The NBD1:NBD2 dimer interface sites that bind ATP and AMP.

(E) The site between ICL4 and NBD1 proximal to the F508del mutation.

(F) Change in F508del NBD1-NBD2 heterodimer interface by the second-site mutation G550E.

(G) Docking of corrector VRT-325 to the ATP site. VRT-325 is shown with gray carbons docked in the ATP site of NBD1-NBD2 heterodimer (transparent dot surface), overlaid on the ATP analog from 3 dg7.pdb (shown with green carbons).

(H) Docking of corrector VX-809 to the F508del-CFTR pocket created at the NBD1:ICL4 interface.

See also Figure S2.

Rescue of F508del-CFTR by Low Temperature Is Additive to Genetic Revertants

To learn more about how low temperature rescues F508del-CFTR, we assessed its combined effect with that of the above genetic revertants: G550E, R1070W, 4RK, V510D, and R555K (Figures 4A and 4B). Results show that low temperature further increases processing levels of F508del-CFTR by the five genetic revertants, namely, V510D, G550E, R1070W, 4RK, and R555K, by an additional 35%, 65%, 38%, 27%,

and 22%, respectively (compare gray and black bars in Figure 4B).

As a negative control, we also analyzed the effect of low temperature on CFTR bearing another class II disease-causing mutation R560T (Roxo-Rosa et al., 2006), confirming its previously described insensitivity to low temperature rescue (Figures 4A and 4B).

These data with revertants again suggest that low temperature configures a different mechanism of rescue, as was the case

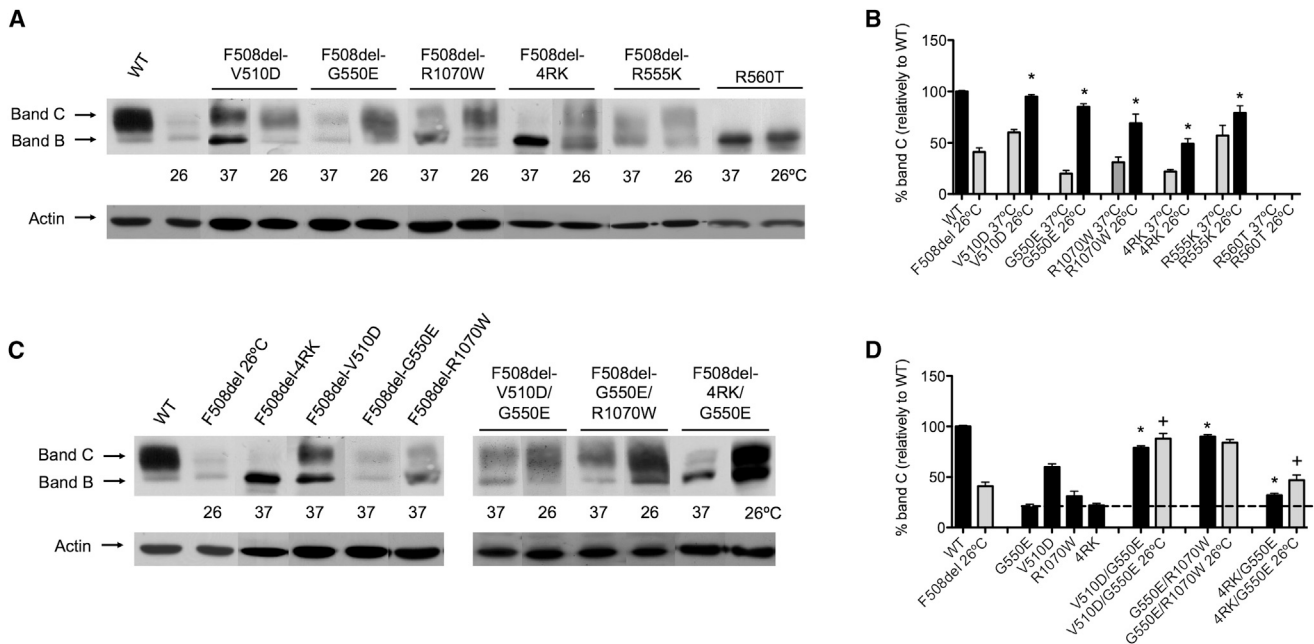


Figure 4. Second-Site Mutations Are Additive to Each Other and Low Temperature in the Rescue of F508del-CFTR

(A) BHK cell lines stably expressing CFTR WT or bearing the mutations indicated were cultured at 37°C or incubated at 26°C for 48 hr as indicated. CFTR protein was analyzed by WB. Data are representative of n = 5–9 experiments.
 (B) For each variant, densitometry was used to calculate the percentage of band C versus total CFTR. This percentage was normalized to WT-CFTR and is shown as mean ± SEM. Asterisks indicate significant difference from the same CFTR variant at 37°C (p < 0.05).
 (C) BHK cell lines stably expressing CFTR WT or different variants were cultured at 37°C or incubated at 26°C for 48 hr as indicated. CFTR protein was analyzed by WB. Data are representative of n = 5–9 experiments.
 (D) For each variant, densitometry was used to calculate the percentage of band C versus total CFTR, as in (B). Asterisks indicate significant difference from single genetic revertants. + indicates significant difference from the same variant at 37°C (p < 0.05). The dotted line corresponds to levels of band C in F508del-G550E-CFTR.

with the correctors. Interestingly, these additive effects were observed not only for revertants promoting protein-autonomous folding (G550E, V510D, and R1070W) but also for the 4RK revertant, which bypasses the AFT-mediated ER retention.

Combination of Different Genetic Revertants Is Also Additive

Next, to assess the full potential for F508del-CFTR rescue, we combined the effects of folding and traffic revertants by producing stable BHK cell lines expressing F508del-G550E-CFTR, where 4RK, V510D, or R1070W were also added in *cis*, and analyzed processing (Figures 4C and 4D). Results in Figure 4C show that 4RK, V510D, and R1070W further increased processing of G550E-F508del-CFTR by another 12%, 59%, and 70%, respectively. In fact, the combined effects of G550E with either V510D or R1070W bring F508del-CFTR processing to ≈80%, i.e., close to levels of WT-CFTR, which can be further increased at 26°C reaching 88%. The combination of G550E with 4RK, although additive, has a more modest effect (32% in total) and is still additive to low temperature (Figure 4D, far right bar).

Low Temperature Kinetics of F508del-CFTR Alone or with 4RK/G550E

The increased effect of combining correctors, revertants, and low temperature is strongly suggestive of different MoAs. However, to further characterize the MoA of low temperature rescue,

we studied the turnover rate and processing efficiency of F508del-CFTR or in *cis* with 4RK/G550E at 26°C in comparison to these variants at 37°C. Pulse-chase experiments followed by CFTR-immunoprecipitation (IP) were thus performed in cells incubated at 26°C and then chased at either 26°C or 37°C (Figure 5A). In parallel, control experiments fully at 37°C were also performed.

Data show that the turnover rate of WT-CFTR band B was substantially decreased when cells were incubated at 26°C and then chased at 37°C (Figure 5A, middle five lanes) in comparison to cells always at 37°C (Figure 5A, first five lanes), and this difference was even more striking when the chase was also at 26°C (Figure 5A, last five lanes). Because this significant decrease in turnover rate of band B (Figure 5B) did not correspond to an increase in its processing, i.e., conversion into the fully-glycosylated band C (Figure 5C), we can conclude that it corresponds to decreased degradation.

The same experiments for F508del-CFTR (Figures 5D and 5E) show that, similarly to WT-CFTR, the turnover rate of immature F508del-CFTR is significantly reduced in cells incubated and chased at 26°C (Figure 5D, last five lanes and Figure 5E), with only the processed form (band C) being barely detectable. However, when the chase was performed at 37°C (Figure 5D, middle five lanes), the turnover rate of band B was similar to that in cells always at 37°C, with no band B being detected, which suggests its rapid degradation once at 37°C.

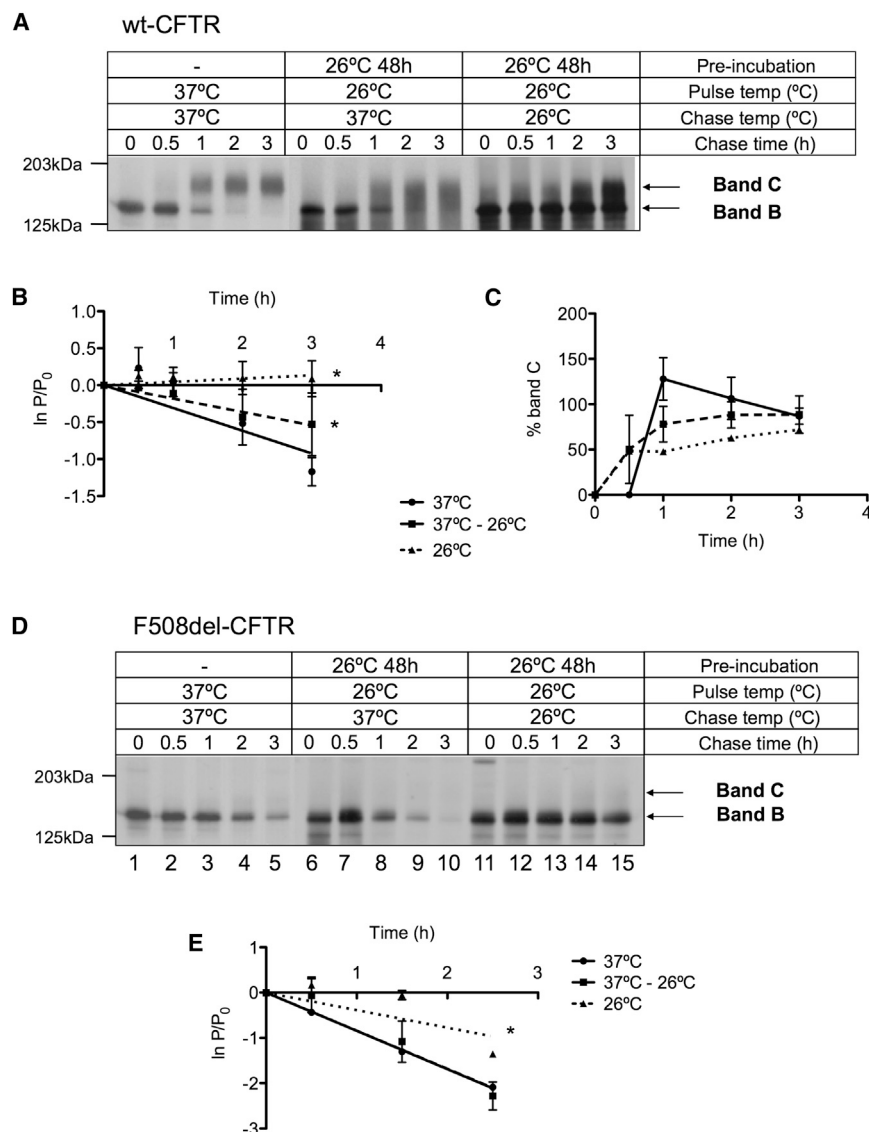


Figure 5. F508del-CFTR Accumulates in Its ER-Specific Immature Form in Cells Incubated at Low Temperature

(A–D) Pulse-chase experiments followed by immunoprecipitation were performed in BHK expressing (A) WT- or (D) F508del-CFTR incubated at 26°C for 48 hr. After labeling at 26°C for 3 hr, chase was performed at either 37°C (middle five lanes) or 26°C (last five lanes). Cells incubated at 37°C and labeled for 30 min at 37°C were also analyzed as a control (first five lanes). Turnover rate of immature form (band B) of (B) WT- or (E) F508del-CFTR was measured as the logarithm of ratio of labeled protein at time t (P_t) to the amount of labeled protein at the start of the chase (P_0). Conversion of the immature form (band B) into the mature form of WT-CFTR (band C) (C) was measured as the percentage of band C at time t relative to the amount of labeled protein at the start of chase. Symbols and error bars are means \pm SEM of $n = 3$ values at each time point. One asterisk indicates the line whose slope is significantly different from that of control line—cells incubated at 37°C ($p < 0.05$). See also Figure S3.

black/stripped bars), the total amount of F508del-4RK-CFTR displays a marked time course decrease either at 26°C (Figure 6B, gray/dotted bars) or at 37°C (Figure 6C, black/stripped bars). The observed results are consistent with CFTR functional data for these variants, as assessed by the iodide (I^-) efflux technique (Figure S4). Altogether they indicate that 4RK is not as additive to low temperature in stabilizing F508del-CFTR as G550E.

Correction of CFTR Bearing Mutants of the Diacidic ER Code

To further dissect the rescue mechanisms of F508del-CFTR rescue by

We then similarly assessed how low temperature affects the turnover and processing of F508del-CFTR bearing the two genetic revertants 4RK and G550E (Figure 6). Results from pulse-chase experiments of F508del-G550E-CFTR show a dramatic reduction in the turnover of the immature form (Figure 6A, left panel), which also corresponds to an increase in its processing efficiency (band C levels) when the chase was performed at 26°C (Figure 6A). Data from similar experiments at 26°C with the 4RK revertant on F508del-CFTR (Figure 6A, right panel) also show that low temperature decreased band B turnover rate, when the chase was performed at 26°C, but only modestly. Interestingly, this effect did not result in an increase in the processing efficiency (Figure 6A, right panel).

The differential behavior observed for F508del-G550E- and F508del-4RK-CFTR at 26°C becomes most evident when these data are plotted as the total amount of band B + band C against time (Figures 6B and 6C). Indeed, whereas the total amount of F508del-G550E-CFTR at 26°C (Figure 6B, gray/dotted bars) only barely decreases in comparison to its total at 37°C (Figure 6B,

VX-809, namely, in relation to ER-to-Golgi traffic, we also tested its rescue effect (as well as that of the other two correctors, low temperature, and genetic revertants) on a CFTR mutant with a defective ER-export DAD-code (Wang et al., 2004).

We first mutated the second residue (Asp567) in the ER DAD-exit code DAA (Figure 7A). As shown previously (Roy et al., 2010), this mutation does not fully abolish CFTR processing, resulting in a $\approx 55\%$ decrease of processing versus WT-CFTR (Figure 7A). We then tested the effect of either correctors or low temperature on this mutant to find that both VX-809 and low temperature increase processed CFTR levels (Figure 7B). Further, AFTs removal from DAA-CFTR (4RK-DAA-CFTR) also increases band C levels (Figure 7B).

Because we aimed to achieve the complete impairment of traffic of WT-CFTR (Wang et al., 2004), we thus generated an additional mutant through abrogation of both Asp565 and Asp567 residues in the DAD-motif of the ER-exit code (DD/AA-CFTR mutant).

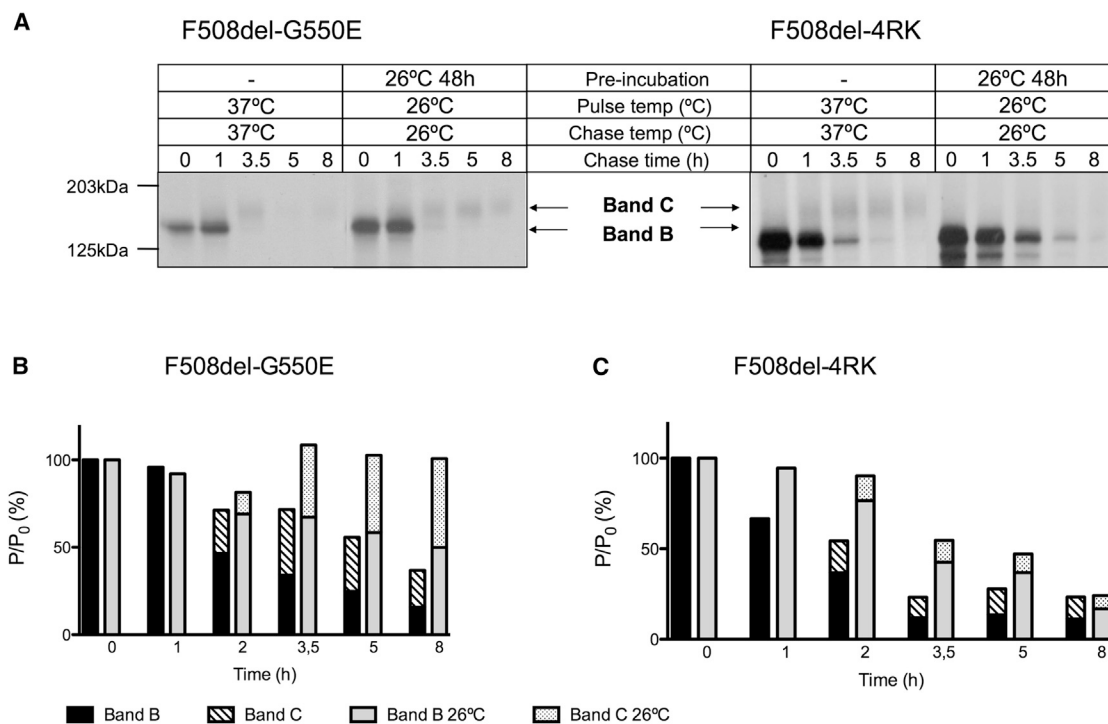


Figure 6. Low Temperature Stabilizes the Immature Form of G550E and 4RK Variants of F508del-CFTR and Acts Synergistically with G550E, but not 4RK, to Rescue F508del-CFTR

(A–C) Pulse-chase experiments followed by IP were performed in BHK cells expressing (A) F508del-G550E (left panel) or F508del-4RK-CFTR (right panel) incubated at 26°C for 48 hr. After labeling with [³⁵S] methionine for 3 hr, chase was performed at 26°C (last five lanes in each panel). The same cells were labeled for 30 min and chased always at 37°C as control (first five lanes). Percentage of bands B and C present at each time point of chase in F508del-G550E- (B) or F508del4RK-CFTR (C) incubated for the duration of the experiment (pulse + chase) at either 26°C or 37°C is shown in graph bars to illustrate the additive effect of low temperature and the genetic revertant G550E, but not 4RK, on F508del-CFTR rescue. Symbols and error bars are means ± SEM of *n* = 5 values at each time point.

See also Figure S4.

As above, cells were incubated with VX-809 (or VRT-325, Corr-4a) or at 26°C (Figures 7C and 7D). Results show that neither VX-809 nor VRT-325 and Corr-4a could rescue DD/AA-CFTR maturation, and interestingly the abrogation of the AFT motifs in this export mutant (DD/AA-4RK-CFTR) was also ineffective. But remarkably, low temperature did rescue the defect caused by elimination of the diacidic code (Figure 7C).

Again, these data were confirmed by the iodide-efflux technique showing that low temperature did indeed rescue ion channel function of DD/AA-CFTR (triangles, Figure 7E) to ≈50% of WT-CFTR (circles, Figure 7E), whereas DD/AA-CFTR cells did not elicit detectable I⁻-efflux (squares, Figure 7E), consistently with its traffic defect and similarly to F508del-CFTR (Figure 7F). A summary of magnitude of peak I⁻-efflux generated by DD/AA-CFTR (Figure 7E) and F508del-CFTR (Figure 7F) expressed as a percentage of WT-CFTR (Figure 7G) shows that low temperature rescues these two variants by ≈50% and ≈40%, respectively, and the difference between these values was found to be statistically significant.

DISCUSSION

The goal of the major corrective therapies for CF, like the investigational drug VX-809, is to rescue the most frequent disease-

causing mutant, F508del-CFTR, to the plasma membrane. Previous studies have shown that this can be achieved by different rescue strategies, namely, (1) by correcting the folding of the mutant protein (either by enhancing NBD1 folding or by promoting interdomain packing) or (2) by releasing the mutant protein from its ER retention through overcoming the barriers imposed by several checkpoints of the ER quality control (Farinha and Amaral, 2005; Rosser et al., 2008; Roxo-Rosa et al., 2006).

Other groups have tested combined treatments to rescue processing of F508del-CFTR (He et al., 2010; Thibodeau et al., 2010). Here, focusing mostly on genetic revertants, but also low temperature and other correctors, we have looked into the investigational drug VX-809 by also comparing and integrating the effects by those various agents in further combinations.

VX-809 Adds to Genetic Revertants and Other Correctors to Rescue F508del-CFTR

Our data show that rescue of F508del-CFTR by VX-809 is additive to that achieved by either genetic revertants or the other correctors (VRT-325 and Corr-4a). These findings strongly suggest distinct MoA for those three compounds but also demonstrate that full correction of F508del-CFTR can be maximized to reach the processing levels of WT-CFTR by using a combination of strategies.

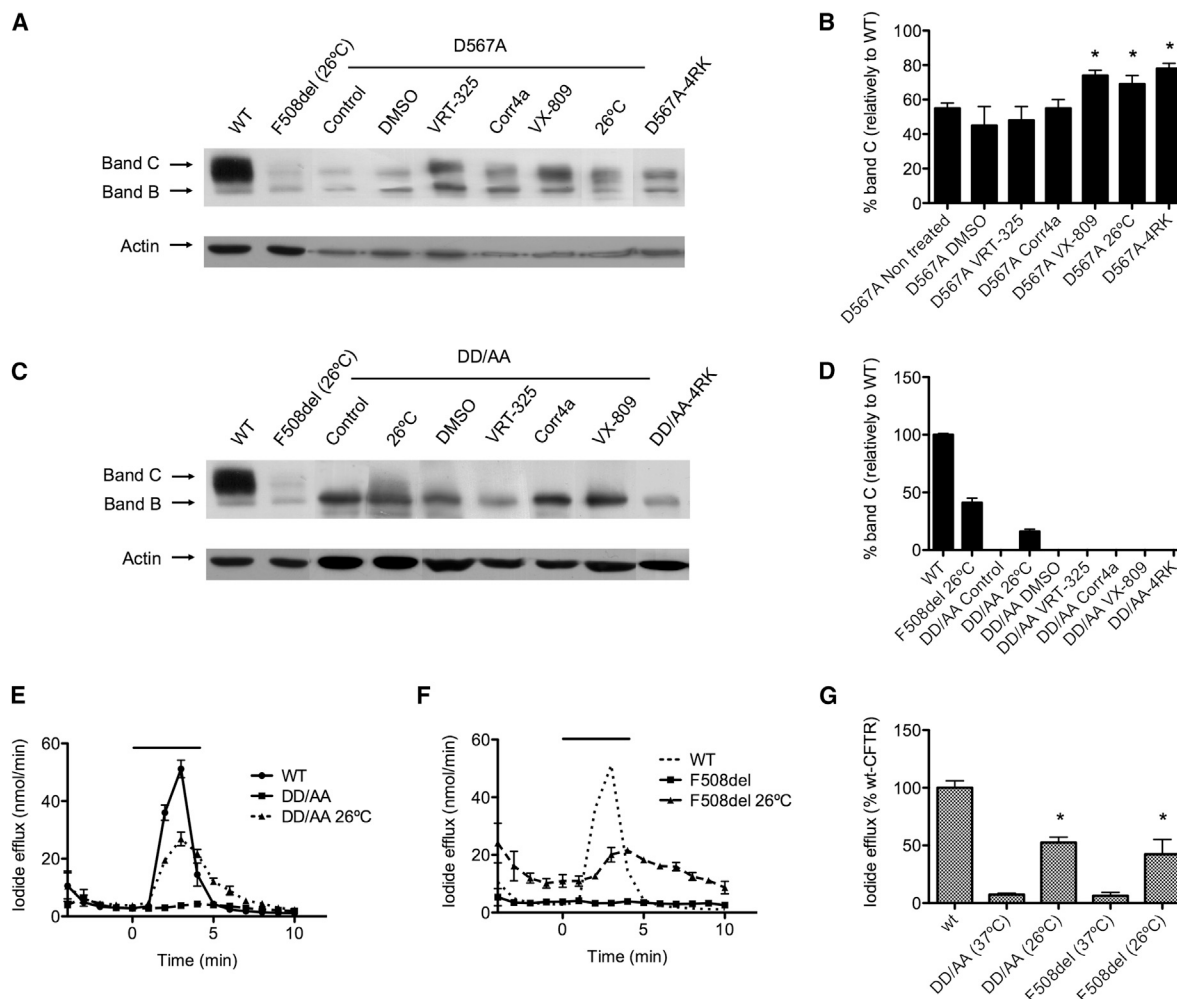


Figure 7. CFTR with Mutated Diacidic Exit Code Is Rescued by Low Temperature, but Not by Correctors

(A) BHK cell lines stably expressing WT-CFTR or bearing the DAA (D567A) mutation alone or in *cis* with 4RK were cultured at 37°C, incubated at 26°C for 48 hr or for 24 hr with VRT-325, Corr-4a, or VX-809, as indicated. CFTR protein was analyzed by WB. Data are representative of $n = 5$ experiments.

(B) For each variant, densitometry was used to calculate the percentage of band C versus total CFTR. This percentage was normalized to WT-CFTR and is shown as mean \pm SEM.

(C) BHK cell lines stably expressing WT-CFTR or bearing the DD/AA mutations (D565A, D567A) alone or in *cis* with 4RK were cultured at 37°C, incubated at 26°C for 48 hr or for 24 hr with VRT-325, Corr-4a, or VX-809, as indicated. CFTR protein was analyzed by WB. Data are representative of $n = 6$ experiments.

(D–F) For each variant, densitometry was used to calculate the percentage of band C versus total CFTR, as in (B). Functional analysis of CFTR variants was assessed by iodide efflux from BHK cells stably expressing (E) WT-, DD/AA- at 37°C and 26°C and (F) WT-, F508del-CFTR at 37°C and 26°C.

(G) Magnitude of peak iodide efflux generated by the different CFTR constructs is determined for each condition as a percentage of WT-CFTR. Symbols and error bars are means \pm SEM of $n = 6$ values at each time point. Asterisks indicate significant difference from respective controls at 37°C ($p < 0.05$).

Importantly, when we analyzed whether VX-809 is additive with revertants known to rescue F508del-CFTR by different mechanisms, we found quite significant differences (Figure 1), which provide clues to the MoA of this compound. Indeed, VX-809 (in contrast to either VRT-325 or Corr-4a) adds to the rescue by G550E and R555K (both acting at the NBD1:NBD2 interface), indicating that the compound and these two revertants probably correct distinct conformational cues of F508del-CFTR. In contrast, the additive effect of VX-809 to R1070W and V510D is rather modest, thus suggesting that this corrector acts more similarly to R1070W/V510D than to G550E/R555K.

VRT-325 in turn (and comparatively to its modest effect alone) significantly increases (by $\approx 29\%$ versus VRT-325 alone) the

rescue efficiency of R1070W and also V510D, suggesting effects at distinct sites.

Potency of correctors (Figures 2A–2C) on revertants showed that compounds act at lower doses than for F508del-CFTR. For example, F508del-G550E-CFTR required a 10-fold lower dose of VX-809 than F508del-CFTR for significant rescue. As proposed before (Thibodeau et al., 2010), F508del-CFTR rescue needs a coordinated effect of both NBD1 correction and interdomain assembly. So, the increased potency of the correctors upon revertants versus F508del-CFTR suggests that an already partially corrected version of the protein (by the revertants in *cis*) is much more easily diverted to a fully corrected conformation—once again, pointing out to the need for

a combined multistep action to more effectively rescue this mutant.

Structural Implications: Putative Correction of the NBD1:ICL4 Interface by VX-809

These observations are further strengthened by our modeling studies, which highlighted two putative contact sites in WT-CFTR that are severely altered in F508del-CFTR and are plausible binding sites for CFTR modulators: one at the NBD1:NBD2 interface and another at the NBD1:ICL4 interface, as previously described (Serohijos et al., 2008). Furthermore, docking and scoring techniques suggest that VX-809 is a good fit for the ICL4 site, whereas VRT-325 is best accommodated by the ATP site (Figures 3G and 3H), and Corr-4a does not fit at either of these sites. This is also consistent with the DSF data showing that none of the three compounds promoted isolated NBD1 folding (Figure S1). Therefore, these compounds should stabilize interdomain interactions: the NBD1:ICL4 interface (VX-809) or the NBD1:NBD2 dimer interface (VRT-325).

However, there is some degree of uncertainty associated with the docking studies and using the final CFTR-folded form may preclude effects by correctors acting on a folding intermediate. Nevertheless, while this paper was under review, others reported similar findings using modeling to elucidate the MoA for VX-809, although allosteric effects could not be excluded as modes of action (He et al., 2013). Importantly, those published data also indicate that VX-809 does not restore the thermodynamic stability of F508del-CFTR, as one would expect for a compound stabilizing a folding intermediate. So, altogether, results from this recent study by He et al. (2013) further support our proposal that VX-809 docks to the NBD1:ICL4 interface. Our findings are also in agreement with recent work from Okiyoneda et al. (2013), who show that VX-809 primarily corrects the destabilization of the NBD1:ICL4 interface caused by absence of F508.

Corr-4a seems to act by an unspecific mechanism as this compound is also able to rescue trafficking mutants of MC4R, melanocortin receptor 4 (J.B.C. Findlay, personal communication), suggesting an unspecific role as a chemical chaperone. In support of this hypothesis, Corr-4a diminished the binding affinity of F508del-NBD1 to the chaperone Hsc70 (Scott-Ward and Amaral, 2009). Also, consistently, Corr-4a acts by a distinct MoA from VRT-325 and VX-809, as there is significant (although modest) synergy between Corr-4a and the other two compounds.

Furthermore, modeling also predicts that revertants G550E and R1070W act at different CFTR interdomain contacts disrupted by F508del: whereas G550E seems to restore the strength of the NBD1:NBD2 interface, R1070W rather promotes the NBD1:ICL4 interaction, as suggested previously (He et al., 2010; Serohijos et al., 2008) and in Figure S2A. Data on combination of the different revertants are fully consistent with this prediction. Indeed, G550E, besides being able to promote rescue of F508del-CFTR (DeCarvalho et al., 2002), shows the largest combined effect with R1070W (or V510D). These data plausibly indicate that correction at both sites is required for full rescue of F508del-CFTR.

Moreover, the observed synergy of G550E or R555K with VX-809, but not VRT-325, is consistent with this model in which VRT-325 acts on the NBD1:NBD2 dimerization interface (also

supported by the synergy between R1070W and VRT-325). Further modeling is, however, required to examine the observation that R1070W is still additive with VX-809 (albeit modestly). This putative effect of VRT-325 is in agreement with its previously reported rescue effect upon P-glycoprotein (Wang et al., 2007c), which also belongs to the ABC transporter superfamily, but not upon mutations in SCN1A, the voltage-gated sodium channel Na(V)1.1, a quite unrelated membrane protein responsible for severe myoclonic epilepsy of infancy (Thompson et al., 2012).

VX-809 and Low Temperature Rescue F508del-CFTR Processing to $\approx 80\%$ of WT-CFTR

Low temperature showed very strong additive effects with VX-809 reaching $\approx 80\%$ of WT-CFTR processing levels. VRT-325 and Corr-4a also added to low temperature but to a lower extent ($\approx 60\%$ of WT-CFTR). These data suggest that low temperature acts on F508del-CFTR differently from the three correctors, and this led us to further investigate its MoA.

We found that at 26°C WT-CFTR significantly accumulates in its immature form, probably due to impairment of pre-Golgi structures to translocate efficiently at this temperature (Lippincott-Schwartz et al., 2000), leading to an accumulation of cargo proteins at the ER exit sites (Presley et al., 1998). F508del-CFTR also accumulates, but once cells are at 37°C, while the ER-accumulated WT-CFTR rapidly traffics to the plasma membrane, most F508del-CFTR is degraded, with only a minor fraction reaching the cell surface (Figure 5). To explain accumulation of the immature form, our results from biosynthesis, trafficking, and degradation of F508del-CFTR at 26°C (Figure S3) confirmed that translation still proceeds, albeit more slowly, whereas proteasomal degradation is reduced as also described (Velickovska et al., 2005). Thus, reduced temperature appears to provide F508del-CFTR a kinetic folding advantage as shown for F508del-NBD1 in vitro (Qu and Thomas, 1996), allowing its accumulation instead of proteasomal degradation. However, such conformation is only intrinsically stable as long as the temperature is low, as suggested by others (Lukacs and Verkman, 2012).

The low maturation levels detected for F508del-CFTR at 26°C incubation (Figure 5D) are probably also derived from its described membrane instability (Lukacs et al., 1993; Sharma et al., 2001). In fact, we recently showed that increasing Rac1 signaling by HGF significantly stabilizes CFTR at the plasma membrane and that treatment with HGF alone rescues F508del-CFTR activity to 10% of WT-CFTR (Moniz et al., 2013). Moreover, HGF adds to VX-809, achieving 30% rescue of the mutant, consistent with the reported inability of VX-809 to restore F508del-CFTR thermodynamic stability (He et al., 2010).

Our data also show that low temperature, similar to chemical correctors, further increases processing levels of F508del-CFTR by the five genetic revertants, although to variable levels: V510D (by an additional 35%), G550E (65%), R1070W (38%), 4RK (27%), and R555K (22%).

The strong synergistic effect of low temperature and G550E on the rescue of F508del-CFTR-efficient processing, but only modestly for 4RK, supported by pulse-chase data, suggest that low temperature and 4RK effects are mechanistically closer to each other (and thus related to bypassing the ER quality control) than low temperature and G550E. This is further supported

by the additive effects of G550E and 4RK effects (Figure 4). Interestingly, others have found that F508del-CFTR associates poorly with Sec24, but this may be reversed by low temperature incubation (Wang et al., 2004), thus providing a further explanation in relation to traffic for the mechanism of this long-known F508del-CFTR rescue strategy (Denning et al., 1992). Although 4RK can also be claimed to impact on F508del-CFTR folding (namely, through its two NBD1 changes: R516K and especially R555K), this is somewhat disproven by the additive effects of 4RK with G550E (Figure 4), the latter truly correcting F508del-NBD1 folding, as assessed by channel gating (Farinha and Amaral, 2005; Rosser et al., 2008; Roxo-Rosa et al., 2006).

VX-809 Enhances DAA Traffic, but Does Not Rescue the Traffic-Deficient Mutant DD/AA

Finally, we tested how VX-809 (as well as VRT-325 and Corr-4a) affected the traffic of diacidic exit code mutants of CFTR. Whereas DAA did not completely abolish processing of CFTR, as previously reported (Roy et al., 2010), VX-809, 4RK, and low temperature further increased its processing levels. Evidence from others suggested DAA-CFTR to be a trafficking mutant without a major conformational defect (Roy et al., 2010). However, the double diacidic mutant DD/AA-CFTR, is the one we found to completely impair appearance of band C. Moreover, this variant was not corrected by any of the compounds tested, suggesting that this trafficking mutant cannot be corrected by pharmacological chaperones. Curiously, the abrogation of the AFT motifs in this export mutant was also ineffective, suggesting the independence of defective ER export and dominant AFT-mediated ER retention mechanisms. As the F508del-CFTR rescue by VX-809 is additive to that of 4RK, it is plausible that this compound does not affect AFT-mediated dominant ER retention.

Very interestingly, however, low temperature could rescue DD/AA-CFTR. This again suggests that low temperature allows this variant to exit the ER, and this should occur through conventional ER-to-Golgi traffic. Indeed, it is highly unlikely that low temperature promotes DD/AA-CFTR ER exit through the recently proposed nonconventional GRASP55-mediated trafficking pathway (Gee et al., 2011), as we show that the temperature-rescued DD/AA-CFTR is fully glycosylated, in contrast to cargo undergoing nonconventional traffic.

Altogether, these data show that VX-809, in contrast to low temperature, cannot overcome the Sec24-COPII-export defect of DD/AA-CFTR.

SIGNIFICANCE

This study highlights the existence of multiple correction mechanisms accounting for the rescue of F508del-CFTR, the most common CF-causing mutant. Assessing the synergistic/additive effects of investigational drug VX-809, one of the most promising to rescue the F508del-CFTR-trafficking defect, with those of genetic revertants as well as other correctors (VRT-325 and Corr-4a) or low temperature pointed to major insights into its MoA: (1) VX-809 is additive to both VRT-325 and Corr-4a, suggesting that each compound operates by a different MoA; (2) VX-809 is additive to low temperature rescue of the mutant almost to WT-CFTR levels; (3) VX-809, VRT-325, and Corr-4a show variable additive effects

with the genetic revertants tested (4RK, G550E, and R1070W), thus providing clues for their possible action being exerted at specific protein binding pockets: VX-809 at the NBD1:TMD2 interface (and VRT-325 at NBD1:NBD2) or acting unspecifically (Corr-4a); and (4) VX-809 does not rescue the diacidic code traffic mutant in contrast to low temperature, which seems to act at trafficking surveillance checkpoints.

Besides suggesting a MoA for VX-809, our data also indicate the scope for further synergistic F508del-CFTR correction by other compounds at distinct conformational sites/cellular checkpoints. Accordingly, they provide a plausible explanation for the limited success of VX-809 in clinical trials, proposing that this compound alone may be insufficient to ascertain clinically relevant CFTR levels at the cell surface. Therefore, combination therapies may be required to achieve complementary rescue by distinct MoA's and full F508del-CFTR correction, so as to reach the functional CFTR threshold necessary to avoid CF. The "best" strategy to bring F508del-CFTR rescue to WT-CFTR functional levels should thus probably involve the combination of several small molecules, each acting on a different step in the complex pathway of F508del-CFTR folding, trafficking, plasma membrane stability, and function. These findings should be exploited for therapeutic strategies of CF.

EXPERIMENTAL PROCEDURES

Cells and Culture Conditions

BHK cell lines expressing F508del-4RK (R29K/R516K/R555K/R716K)-, F508del-G550E-, F508del-R1070W-, F508del-V510D-, F508del-R555K-, F508del-V510D/G550E-, F508del-G550E/R1070W-, DAA (D567A)-, 4RK-DAA-, DD/AA (D565A, D567A)-, 4RK-DD/AA-, and R560T-CFTR were produced and cultured as previously described (Roxo-Rosa et al., 2006). For low temperature experiments, cells were incubated at 26°C for the indicated periods of time. The small molecule correctors VRT-325 (Wang et al., 2007b) used at 6.7 μM and Corr-4a (Pedemonte et al., 2005) used at 10 μM were obtained through Cystic Fibrosis Foundation Therapeutics. VX-809 was obtained from Selleck Chemicals and used at 3 μM for 24 hr (Van Goor et al., 2011). For potency tests, cells were incubated for 24 hr with VRT-325: 6.7 nM, 67 nM, 670 nM, 1.0 μM, 6.7 μM, or 20 μM; Corr4a: 1.0 nM, 10 nM, 100 nM, 1.0 μM, 10 μM, or 25 μM; or VX-809: 3.0 nM, 30 nM, 300 nM, 3.0 μM, 10 μM, or 30 μM. As vehicle control, cells were also incubated with DMSO alone at the same concentration used when in presence of correctors, i.e., 0.1% (v/v), and this was used as the baseline control.

CFTR Homology Model

Our model was based on the alignment of human CFTR sequence (MSDs and NBDs) with the *Staphylococcus aureus* Sav1866 sequence, to preserve the interface features between the different domains and on the published structure of this bacterial ABC transporter (Hohl et al., 2012).

NBD1/NBD2 heterodimer was constructed by overlay using sequence and secondary structure of NBD2 from 3DF7 with the heterodimer structure of F508del 2PZE (Atwell et al., 2010).

Modeling was performed as a whole using MOE software from the Chemical Computing Group (*Molecular Operating Environment [MOE]*, 2011.10; Chemical Computing Group). For investigation of putative binding sites for compounds on the monomeric NBD1 and the dimeric NBD1/NBD2, we used ligand binding site finding algorithm *Q-SiteFinder* (Laurie and Jackson, 2005).

Western Blot

To probe for the effect of low temperature, genetics revertants, and compounds upon CFTR processing by western blot (WB), cells were incubated with each compound at a chosen concentration for 24 hr at either 37°C or 26°C, as indicated. After incubation, cells were lysed and extracts analyzed

as described previously (Farinha et al., 2002) using the anti-CFTR antibody 596 (CFF). Percentage of band C to total CFTR was calculated by normalizing the ratio of band C/total CFTR (bands B+C) relatively to the same ratio in samples from WT-CFTR expressing cells as a control.

Pulse-Chase and Immunoprecipitation

After incubation at 26°C, cells expressing CFTR were starved for 30 min in methionine-free medium and then pulsed for 30 min at 37°C or for 3 hr at 26°C in the same medium supplemented with 150 μ Ci [³⁵S]methionine. Pulse-chase experiments, followed by immunoprecipitation of CFTR were performed as previously described (Farinha et al., 2002).

Iodide Efflux

CFTR-mediated iodide efflux was measured at room temperature using the cAMP agonist forskolin (10 μ M) and the CFTR potentiator genistein (50 μ M; Sigma-Aldrich) as described previously (Lansdell et al., 1998; Roxo-Rosa et al., 2006).

Statistical Analysis

Quantitative results are shown as means \pm SEM of *n* observations. To compare two sets of data, we used Student's *t* test when differences are significant for *p* values < 0.05.

Differential Scanning Fluorimetry

The effect of small compounds on the thermal stability of murine WT- and F508del-NBD1 was evaluated through DSF (Lavinder et al., 2009; Senisterra and Finerty, 2009). Briefly, the different compound solutions were distributed into PCR plates (Bio-Rad), and protein solution with Sypro Orange 5-fold (Invitrogen) was added to each well. Plates were sealed with optical quality sealing tape (Bio-Rad) and run in an iCycler iQ Real-Time thermocycler instrument (Bio-Rad) using an excitation filter from 530 to 560 nm and an emission filter from 575 to 595 nm. Temperature was increased from 20°C to 90°C, with increments of 2°C.min⁻¹. The fits of the unfolding transitions were carried out using Origin (MicroCal) assuming a two-state model. For each condition, the midpoint transitions (melting temperatures, *T_m*) were determined (Pace et al., 1998). Protein concentration was 4 μ M in the case of the wild-type NBD1 and 6 μ M for NBD1-F508del. Experiments were performed in 20 mM sodium phosphate (pH 7.4) and 1 mM DTT.

SUPPLEMENTAL INFORMATION

Supplemental Information includes four figures and one table and can be found with this article online at <http://dx.doi.org/10.1016/j.chembiol.2013.06.004>.

ACKNOWLEDGMENTS

Our work was supported by strategic grants (PEst-OE/BIA/UI4046/2011, BioFIG; PEst-OE/EQB/LA0004/2011, ITQB), grants from FCT, Portugal (PTDC/BIA-BCM/112635/2009 to C.M.F. and PTDC/SAU-GMG/122299/2010 to M.D.A.), grants from the European Union (TargetScreen2 EU-LSH-2005-1.2.5-3-037365), and a grant from the CFF-Cystic Fibrosis Foundation (ref. 7207534 to M.D.A.). We thank CFF-USA for correctors (B. Bridges), anti-CFTR 596 antibody (J.R. Riordan), and purified murine WT- and F508del-NBD1 (P.J. Thomas). We also thank Dr. Luka Clarke (BioFIG) for reviewing this manuscript. M.S. and B.J.H. received fellowships from FCT (SFRH/BD/35936/2007 and SFRH/BPD/74475/2010). J.W. and S.H. are employees and shareholders of Sygnature Discovery.

Received: August 3, 2012

Revised: May 10, 2013

Accepted: June 9, 2013

Published: July 25, 2013

REFERENCES

Amaral, M.D. (2004). CFTR and chaperones: processing and degradation. *J. Mol. Neurosci.* 23, 41–48.

Amaral, M.D. (2011). Targeting CFTR: how to treat cystic fibrosis by CFTR-repairing therapies. *Curr. Drug Targets* 12, 683–693.

Atwell, S., Brouillette, C.G., Conners, K., Emtage, S., Gheyi, T., Guggino, W.B., Hendle, J., Hunt, J.F., Lewis, H.A., Lu, F., et al. (2010). Structures of a minimal human CFTR first nucleotide-binding domain as a monomer, head-to-tail homodimer, and pathogenic mutant. *Protein Eng. Des. Sel.* 23, 375–384.

Chang, X.B., Cui, L., Hou, Y.X., Jensen, T.J., Aleksandrov, A.A., Mengos, A., and Riordan, J.R. (1999). Removal of multiple arginine-framed trafficking signals overcomes misprocessing of delta F508 CFTR present in most patients with cystic fibrosis. *Mol. Cell* 4, 137–142.

Clancy, J.P., Rowe, S.M., Accurso, F.J., Aitken, M.L., Amin, R.S., Ashlock, M.A., Ballmann, M., Boyle, M.P., Bronsveld, I., Campbell, P.W., et al. (2012). Results of a phase IIa study of VX-809, an investigational CFTR corrector compound, in subjects with cystic fibrosis homozygous for the F508del-CFTR mutation. *Thorax* 67, 12–18.

Dalemans, W., Barbry, P., Champigny, G., Jallat, S., Dott, K., Dreyer, D., Crystal, R.G., Pavirani, A., Lecocq, J.P., and Lazdunski, M. (1991). Altered chloride ion channel kinetics associated with the delta F508 cystic fibrosis mutation. *Nature* 354, 526–528.

DeCarvalho, A.C., Gansheroff, L.J., and Teem, J.L. (2002). Mutations in the nucleotide binding domain 1 signature motif region rescue processing and functional defects of cystic fibrosis transmembrane conductance regulator delta f508. *J. Biol. Chem.* 277, 35896–35905.

Denning, G.M., Anderson, M.P., Amara, J.F., Marshall, J., Smith, A.E., and Welsh, M.J. (1992). Processing of mutant cystic fibrosis transmembrane conductance regulator is temperature-sensitive. *Nature* 358, 761–764.

Farinha, C.M., and Amaral, M.D. (2005). Most F508del-CFTR is targeted to degradation at an early folding checkpoint and independently of calnexin. *Mol. Cell Biol.* 25, 5242–5252.

Farinha, C.M., Nogueira, P., Mendes, F., Penque, D., and Amaral, M.D. (2002). The human DnaJ homologue (Hdj)-1/heat-shock protein (Hsp) 40 co-chaperone is required for the in vivo stabilization of the cystic fibrosis transmembrane conductance regulator by Hsp70. *Biochem. J.* 366, 797–806.

Gee, H.Y., Noh, S.H., Tang, B.L., Kim, K.H., and Lee, M.G. (2011). Rescue of Δ F508-CFTR trafficking via a GRASP-dependent unconventional secretion pathway. *Cell* 146, 746–760.

Grove, D.E., Rosser, M.F., Ren, H.Y., Naren, A.P., and Cyr, D.M. (2009). Mechanisms for rescue of correctable folding defects in CFTRDelta F508. *Mol. Biol. Cell* 20, 4059–4069.

He, L., Aleksandrov, L.A., Cui, L., Jensen, T.J., Nesbitt, K.L., and Riordan, J.R. (2010). Restoration of domain folding and interdomain assembly by second-site suppressors of the DeltaF508 mutation in CFTR. *FASEB J.* 24, 3103–3112.

He, L., Kota, P., Aleksandrov, A.A., Cui, L., Jensen, T., Dokholyan, N.V., and Riordan, J.R. (2013). Correctors of Δ F508 CFTR restore global conformational maturation without thermally stabilizing the mutant protein. *FASEB J.* 27, 536–545.

Hohl, M., Briand, C., Grütter, M.G., and Seeger, M.A. (2012). Crystal structure of a heterodimeric ABC transporter in its inward-facing conformation. *Nat. Struct. Mol. Biol.* 19, 395–402.

Jensen, T.J., Loo, M.A., Pind, S., Williams, D.B., Goldberg, A.L., and Riordan, J.R. (1995). Multiple proteolytic systems, including the proteasome, contribute to CFTR processing. *Cell* 83, 129–135.

Lansdell, K.A., Kidd, J.F., Delaney, S.J., Wainwright, B.J., and Sheppard, D.N. (1998). Regulation of murine cystic fibrosis transmembrane conductance regulator Cl⁻ channels expressed in Chinese hamster ovary cells. *J. Physiol.* 512, 751–764.

Laurie, A.T., and Jackson, R.M. (2005). Q-SiteFinder: an energy-based method for the prediction of protein-ligand binding sites. *Bioinformatics* 21, 1908–1916.

Lavinder, J.J., Hari, S.B., Sullivan, B.J., and Magliery, T.J. (2009). High-throughput thermal scanning: a general, rapid dye-binding thermal shift screen for protein engineering. *J. Am. Chem. Soc.* 131, 3794–3795.

Lewis, H.A., Wang, C., Zhao, X., Hamuro, Y., Conners, K., Kearns, M.C., Lu, F., Sauder, J.M., Molnar, K.S., Coales, S.J., et al. (2010). Structure and dynamics

- of NBD1 from CFTR characterized using crystallography and hydrogen/deuterium exchange mass spectrometry. *J. Mol. Biol.* **396**, 406–430.
- Lippincott-Schwartz, J., Roberts, T.H., and Hirschberg, K. (2000). Secretory protein trafficking and organelle dynamics in living cells. *Annu. Rev. Cell Dev. Biol.* **16**, 557–589.
- Loo, T.W., Bartlett, M.C., and Clarke, D.M. (2005). Rescue of DeltaF508 and other misprocessed CFTR mutants by a novel quinazoline compound. *Mol. Pharm.* **2**, 407–413.
- Loo, T.W., Bartlett, M.C., and Clarke, D.M. (2010). The V510D suppressor mutation stabilizes DeltaF508-CFTR at the cell surface. *Biochemistry* **49**, 6352–6357.
- Lukacs, G.L., and Verkman, A.S. (2012). CFTR: folding, misfolding and correcting the Δ F508 conformational defect. *Trends Mol. Med.* **18**, 81–91.
- Lukacs, G.L., Chang, X.B., Bear, C., Kartner, N., Mohamed, A., Riordan, J.R., and Grinstein, S. (1993). The delta F508 mutation decreases the stability of cystic fibrosis transmembrane conductance regulator in the plasma membrane. Determination of functional half-lives on transfected cells. *J. Biol. Chem.* **268**, 21592–21598.
- Moniz, S., Sousa, M., Moraes, B.J., Mendes, A.I., Palma, M., Barreto, C., Fragata, J.I., Amaral, M.D., and Matos, P. (2013). HGF stimulation of Rac1 signaling enhances pharmacological correction of the most prevalent cystic fibrosis mutant F508del-CFTR. *ACS Chem. Biol.* **8**, 432–442.
- Niesen, F.H., Berglund, H., and Vedadi, M. (2007). The use of differential scanning fluorimetry to detect ligand interactions that promote protein stability. *Nat. Protoc.* **2**, 2212–2221.
- Nishimura, N., and Balch, W.E. (1997). A di-acidic signal required for selective export from the endoplasmic reticulum. *Science* **277**, 556–558.
- Okiyoneda, T., Veit, G., Dekkers, J.F., Bagdany, M., Soya, N., Xu, H., Roldan, A., Verkman, A.S., Kurth, M., Simon, A., et al. (2013). Mechanism-based corrector combination restores DeltaF508-CFTR folding and function. *Nat. Chem. Biol.* **9**, 444–454.
- Pace, C.N., Hebert, E.J., Shaw, K.L., Schell, D., Both, V., Krajcikova, D., Sevcik, J., Wilson, K.S., Dauter, Z., Hartley, R.W., and Grimsley, G.R. (1998). Conformational stability and thermodynamics of folding of ribonucleases Sa, Sa2 and Sa3. *J. Mol. Biol.* **279**, 271–286.
- Pedemonte, N., Lukacs, G.L., Du, K., Caci, E., Zegarra-Moran, O., Galletta, L.J., and Verkman, A.S. (2005). Small-molecule correctors of defective DeltaF508-CFTR cellular processing identified by high-throughput screening. *J. Clin. Invest.* **115**, 2564–2571.
- Pissarra, L.S., Farinha, C.M., Xu, Z., Schmidt, A., Thibodeau, P.H., Cai, Z., Thomas, P.J., Sheppard, D.N., and Amaral, M.D. (2008). Solubilizing mutations used to crystallize one CFTR domain attenuate the trafficking and channel defects caused by the major cystic fibrosis mutation. *Chem. Biol.* **15**, 62–69.
- Presley, J.F., Smith, C., Hirschberg, K., Miller, C., Cole, N.B., Zaal, K.J., and Lippincott-Schwartz, J. (1998). Golgi membrane dynamics. *Mol. Biol. Cell* **9**, 1617–1626.
- Qu, B.H., and Thomas, P.J. (1996). Alteration of the cystic fibrosis transmembrane conductance regulator folding pathway. *J. Biol. Chem.* **271**, 7261–7264.
- Riordan, J.R. (2008). CFTR function and prospects for therapy. *Annu. Rev. Biochem.* **77**, 701–726.
- Riordan, J.R., Rommens, J.M., Kerem, B., Alon, N., Rozmahel, R., Grzelczak, Z., Zielenski, J., Lok, S., Plavsic, N., Chou, J.L., et al. (1989). Identification of the cystic fibrosis gene: cloning and characterization of complementary DNA. *Science* **245**, 1066–1073.
- Rosser, M.F., Grove, D.E., Chen, L., and Cyr, D.M. (2008). Assembly and misassembly of cystic fibrosis transmembrane conductance regulator: folding defects caused by deletion of F508 occur before and after the calnexin-dependent association of membrane spanning domain (MSD) 1 and MSD2. *Mol. Biol. Cell* **19**, 4570–4579.
- Roxo-Rosa, M., Xu, Z., Schmidt, A., Neto, M., Cai, Z., Soares, C.M., Sheppard, D.N., and Amaral, M.D. (2006). Revertant mutants G550E and 4RK rescue cystic fibrosis mutants in the first nucleotide-binding domain of CFTR by different mechanisms. *Proc. Natl. Acad. Sci. USA* **103**, 17891–17896.
- Roy, G., Chalfin, E.M., Saxena, A., and Wang, X. (2010). Interplay between ER exit code and domain conformation in CFTR misprocessing and rescue. *Mol. Biol. Cell* **21**, 597–609.
- Scott-Ward, T.S., and Amaral, M.D. (2009). Deletion of Phe508 in the first nucleotide-binding domain of the cystic fibrosis transmembrane conductance regulator increases its affinity for the heat shock cognate 70 chaperone. *FEBS J.* **276**, 7097–7109.
- Senisterra, G.A., and Finerty, P.J., Jr. (2009). High throughput methods of assessing protein stability and aggregation. *Mol. Biosyst.* **5**, 217–223.
- Serohijos, A.W., Hegedus, T., Aleksandrov, A.A., He, L., Cui, L., Dokholyan, N.V., and Riordan, J.R. (2008). Phenylalanine-508 mediates a cytoplasmic-membrane domain contact in the CFTR 3D structure crucial to assembly and channel function. *Proc. Natl. Acad. Sci. USA* **105**, 3256–3261.
- Sharma, M., Benharouga, M., Hu, W., and Lukacs, G.L. (2001). Conformational and temperature-sensitive stability defects of the delta F508 cystic fibrosis transmembrane conductance regulator in post-endoplasmic reticulum compartments. *J. Biol. Chem.* **276**, 8942–8950.
- Sharma, M., Pampinella, F., Nemes, C., Benharouga, M., So, J., Du, K., Bache, K.G., Papsin, B., Zerangue, N., Stenmark, H., and Lukacs, G.L. (2004). Misfolding diverts CFTR from recycling to degradation: quality control at early endosomes. *J. Cell Biol.* **164**, 923–933.
- Swiatecka-Urban, A., Brown, A., Moreau-Marquis, S., Renuka, J., Coutermarsh, B., Barnaby, R., Karlson, K.H., Flotte, T.R., Fukuda, M., Langford, G.M., and Stanton, B.A. (2005). The short apical membrane half-life of rescued DeltaF508-cystic fibrosis transmembrane conductance regulator (CFTR) results from accelerated endocytosis of DeltaF508-CFTR in polarized human airway epithelial cells. *J. Biol. Chem.* **280**, 36762–36772.
- Thibodeau, P.H., Richardson, J.M., 3rd, Wang, W., Millen, L., Watson, J.M., Mendoza, J.L., Du, K., Fischman, S., Senderowitz, H., Lukacs, G.L., et al. (2010). The cystic fibrosis-causing mutation deltaF508 affects multiple steps in cystic fibrosis transmembrane conductance regulator biogenesis. *J. Biol. Chem.* **285**, 35825–35835.
- Thompson, C.H., Porter, J.C., Kahlig, K.M., Daniels, M.A., and George, A.L., Jr. (2012). Nontruncating SCN1A mutations associated with severe myoclonic epilepsy of infancy impair cell surface expression. *J. Biol. Chem.* **287**, 42001–42008.
- Van Goor, F., Hadida, S., Grootenhuys, P.D., Burton, B., Stack, J.H., Straley, K.S., Decker, C.J., Miller, M., McCartney, J., Olson, E.R., et al. (2011). Correction of the F508del-CFTR protein processing defect in vitro by the investigational drug VX-809. *Proc. Natl. Acad. Sci. USA* **108**, 18843–18848.
- Varga, K., Goldstein, R.F., Jurkuvenaite, A., Chen, L., Matalon, S., Sorscher, E.J., Bebok, Z., and Collawn, J.F. (2008). Enhanced cell-surface stability of rescued DeltaF508 cystic fibrosis transmembrane conductance regulator (CFTR) by pharmacological chaperones. *Biochem. J.* **410**, 555–564.
- Velickovska, V., Lloyd, B.P., Qureshi, S., and van Breukelen, F. (2005). Proteolysis is depressed during torpor in hibernators at the level of the 20S core protease. *J. Comp. Physiol. B* **175**, 329–335.
- Wang, X., Matteson, J., An, Y., Moyer, B., Yoo, J.S., Bannykh, S., Wilson, I.A., Riordan, J.R., and Balch, W.E. (2004). COPII-dependent export of cystic fibrosis transmembrane conductance regulator from the ER uses a di-acidic exit code. *J. Cell Biol.* **167**, 65–74.
- Wang, Y., Loo, T.W., Bartlett, M.C., and Clarke, D.M. (2007a). Additive effect of multiple pharmacological chaperones on maturation of CFTR processing mutants. *Biochem. J.* **406**, 257–263.
- Wang, Y., Loo, T.W., Bartlett, M.C., and Clarke, D.M. (2007b). Correctors promote maturation of cystic fibrosis transmembrane conductance regulator (CFTR)-processing mutants by binding to the protein. *J. Biol. Chem.* **282**, 33247–33251.
- Wang, Y., Loo, T.W., Bartlett, M.C., and Clarke, D.M. (2007c). Modulating the folding of P-glycoprotein and cystic fibrosis transmembrane conductance regulator truncation mutants with pharmacological chaperones. *Mol. Pharmacol.* **71**, 751–758.